Reflection and transmission of light at periodic layered metamaterial films

Thomas Paul, C. Menzel, Wojciech Śmigaj, C. Rockstuhl, Philippe Lalanne, F. Lederer

Reflection and transmission of light at periodic layered metamaterial films

Thomas Paul,[1,*] Christoph Menzel,[1] Wojciech Śmigaj,[2] Carsten Rockstuhl,[1] Philippe Lalanne,[2,†] and Falk Lederer[1]

[1]*Institute of Condensed Matter Theory and Solid State Optics, Abbe Center of Photonics, Friedrich-Schiller-Universität Jena, Max-Wien-Platz 1, DE-07743 Jena, Germany*

[2]*Laboratoire Charles Fabry de l'Institut d'Optique, CNRS, Université Paris-Sud, Campus Polytechnique, RD 128, FR-91127 Palaiseau, France*

(Received 29 April 2011; revised manuscript received 26 July 2011; published 26 September 2011)

The appropriate description of light scattering (transmission/reflection) at a bulky artificial medium, consisting of a sequence of functional metamaterial and natural material films, represents a major challenge in current theoretical nano-optics. Because in many relevant cases, in particular, in the optical domain, a metamaterial must not be described by an effective permittivity and permeability the usual Fresnel formalism cannot be applied. A reliable alternative consists in using a Bloch mode formalism known, e.g., from the theory of photonic crystals. It permits to split this complex issue into two more elementary ones, namely the study of light propagation in an infinitely extended metamaterial and the analysis of light scattering at interfaces between adjacent meta and natural materials. The first problem is routinely solved by calculating the relevant Bloch modes and their dispersion relations. The second task is more involved and represents the subject of the present study. It consists in using the general Bloch mode orthogonality to derive rigorous expressions for the reflection and transmission coefficients at an interface between two three-dimensional absorptive periodic media for arbitrary incidence. A considerable simplification can be achieved if only the fundamental Bloch modes of both media govern the scattering properties at the interface. If this approximation is valid, which depends on the longitudinal metamaterial period, the periodic metamaterial may be termed homogeneous. Only in this case the disentanglement of the fundamental modes of both media can be performed and the reflection/transmission coefficients can be expressed in terms of two impedances, each depending solely on the properties of the fundamental mode of the respective medium. In order to complement the picture, we apply the present formalism to the quite general problem of reflection/transmission at a metamaterial film sandwiched between a dissimilar metamaterial. This situation asks for a devoted treatment where multiple modes have to be taken into account.

DOI: 10.1103/PhysRevB.84.115142 PACS number(s): 78.20.Ci, 78.20.Bh, 78.67.Pt, 42.25.Bs

I. INTRODUCTION

The desire for media exhibiting strong dispersion in permeability and/or permittivity was driven by proposals for spectacular applications as the perfect lens or the cloaking device, being only one example from the prosperous field of transformation optics.[1–8] These properties came in sight by taking advantage of metamaterials (MMs). MMs are mostly made of periodically arranged subwavelength unit cells termed meta-atoms. Common sense suggests that effective properties may be assigned to MMs if light does not resolve the spatial details of the unit cells but experiences instead an effective homogenous medium characterized, most generally, by bianisotropic constitutive relations containing the effective material parameters: permeability, permittivity, and electromagnetic coupling parameter. These material parameters must be necessarily independent of the shape and the illumination scheme of a specimen and are solely related to the material itself.[9] However, it has been shown recently[10] that in the optical domain this assignment is not permitted for typical MMs due to the mesoscopic size of the meta-atoms. Since most interesting dispersive features of MMs fade away as the size of their unit cell is reduced beyond a certain limit,[10–14] one has to get used to the fact that operation in the mesoscopic domain is rather unavoidable. However, in recent publications, the term "homogeneity" with regard to metamaterials has been discussed in a broader context[15–17] based on the optical response (scattering response) of a specific MM. Thus it is not surprising that a unifying solution for a possible homogenization of all kinds of MMs, in particular such containing mesoscopic structures, does not exist. Here, we focus on MMs consisting of a sequence of functional layers (stack of monolayers with periodically arranged meta-atoms sandwiched between dielectric spacers) where the lateral period is only a few times less than the wavelength. This situation is typical for MMs operated in the optical domain.

In our further consideration, we will leave aside the trivial cases of a genuine homogeneous (unstructured crystalline or amorphous) or an effective homogenous medium (size of inclusions much less than the wavelength) where material parameters can be assigned. We will rather define homogeneity in a broader context as mentioned above. It might be best understood in terms of a hierarchical scheme, where subsequent statements require the previous ones to be fulfilled. (1) The period of the arrangement of unit cells (meta-atoms) has to be sufficiently small in order to guarantee that nonzero diffraction orders of a sample are evanescent. (2) Light propagation inside the medium as well as the coupling of light from or to an adjacent medium is governed by the fundamental Bloch mode (FM) with its respective dispersion relation. In the following, this case is called the fundamental mode approximation (FMA).[18] (3) In FMA, light propagation and scattering is then characterized by the longitudinal wave vector component of this mode, derived from the dispersion relation and henceforth termed propagation constant and an impedance, usually called Bloch impedance.[19,20] These two

parameters are sometimes referred to as "wave parameters." If these conditions are met, we will term the periodically structured medium homogeneous. The final stage of an effective homogeneous medium is approached if the dispersion relation of the FM coincides with that of a medium obeying definite constitutive relations. The wave parameters might then be mapped onto material parameters (permittivity, permeability, and electromagnetic coupling parameter).

In view of the above classification, there are two key questions arising, namely, (i) when is the FMA valid and (ii) which approach can be applied beyond its applicability likewise serving as a benchmark. The answer to both questions requires a more fundamental description of light scattering at MMs. As known from the theory of photonic crystals, a Bloch modal approach is the natural choice when dealing with periodic media (see, for example, Ref. 21). However, there is always a trade off between sufficient predictive power and simplicity such that light interaction with MMs does not always require a rigorous solution to Maxwell's equations. Just to resolve this issue will be the subject of the present contribution.

It has been shown that light propagation inside a bulk MM can be described based on the concept of Bloch modes.[22–24] In principle, it requires to deal with an infinite number of modes, which are usually calculated by numerical means.[25–27] At first glance, this approach does not simplify the problem but it has been shown that the least damped Bloch mode—the so-called fundamental mode—describes light propagation in most bulk MMs sufficiently well.[18] This reduces the propagation issue to the evolution of a single mode in full analogy to a plane wave propagating in a genuine homogeneous medium. Most optical properties of a bulk MM can be fully extracted from the dispersion relation of that single mode, e.g., beam refraction or diffraction[17,28] or pulse spreading. In this context, it has been shown that a left-handed behavior is neither a sufficient nor a necessary condition to achieve negative refraction or anomalous diffraction.[17]

Now, shifting the focus from infinite MMs toward finite thicknesses, the scattering (reflection and transmission) properties of MMs become important to be considered. Detrimental for a description of finite structures, e.g., a slab or stratified MMs, is the potential excitation of a larger number of Bloch modes at the interfaces. Then, the coupling of light into the MM is a complicated issue and requires a devoted rigorous treatment.[29] It would be highly desirable to likewise simplify this treatment and, preferably, to extract the coupling properties of the MM interface from that Bloch mode that dominates the light propagation in the bulk. Along these lines we have recently shown that coupling between two nanostructured media can be sufficiently well described by a single mode in both media, as long as their geometrical differences are small.[30]

Here, we extend this approach to the general case of light reflection and transmission at a single, planar interface between strongly dissimilar MMs under generally oblique incidence. To put it briefly, we will derive rigorous as well as approximate (FMA) algebraic expressions for the reflection and transmission coefficients in terms of the Bloch modes of both media. Then, by concentrating on the rather special but highly relevant case of the single interface between vacuum and an MM, we will evaluate the limits of the FMA. Finally, we will go beyond this scenario in discussing an example that requires the most general treatment, i.e., when reflection and transmission are governed by multiple modes.

Accordingly, the manuscript is structured as follows. In Sec. II, we will discuss the very general problem of coupling obliquely incident light from one semiinfinite MM to another one. Mode coupling at the interface of two different periodic media, as, e.g., photonic crystals, has been already considered prior to the present work. In this context, various approaches have been proposed by the assignment of impedances or impedance matrices,[31–36] but except of our recent works,[24,30] most earlier works dealt with nonabsorbing and two-dimensional media. In contrast to that, our approach, which is based on Bloch mode orthogonality, is valid for three-dimensional structures even in the strongly absorbing regime. Using these relations, we will end up with closed-form expressions for the reflection/transmission coefficients in terms of Bloch modes of both MMs. We will then outline an approximation that takes into account only a finite number of modes in each MM, ideally only a single one. This potentially allows for an appreciable simplification of the model and thus may be useful in the future design of functional MM elements. Eventually, the reflection/transmission problem at an arbitrary stack consisting of meta and natural materials can serve as an example. It is thus straightforward to implement an algorithm using 2×2 matrices that stays in full analogy to the well-established simple matrix approach for natural material stacks.

In Sec. III, we will apply our findings to the scattering at an interface between a homogeneous dielectric medium and an MM. Based on this scenario, we will evaluate the level of homogeneity of a certain bulky MM. In doing so, we will show that the present approach is very close to the introduction of an impedance—in several articles designated as the Bloch impedance—which is defined as the ratio between tangential electrical and magnetic fields.[19,20,35] Most notably we show here that an MM, which exhibits a minimum longitudinal period required for homogenization, still supports the dispersive effects of interest, i.e., a left-handed behavior.

The contribution is signed off with two further sections. In Sec. IV, we numerically study the scattering at a bulky Swiss cross MM film sandwiched between a fishnet MM. It turns out, that the FMA fails in this case. Instead, by taking into account several (evanescent) Bloch modes, the reflection and transmission coefficients can be observed to converge against the rigorous solutions. Finally, we will sum up our findings in Sec. V and discuss the implications of our contribution.

II. INTERFACE BETWEEN TWO DISSIMILAR METAMATERIALS: THEORETICAL TREATMENT

A. General description

The general problem of light scattering at the interface between two periodic media $\mathcal{L}$ (left) and $\mathcal{R}$ (right) under oblique incidence is displayed in Fig. 1.

The eigenmodes at either side of the interface are Bloch modes. In the following derivation, we will assume monochromatic fields proportional to $\exp(-i\omega t)$ with a real frequency ω.

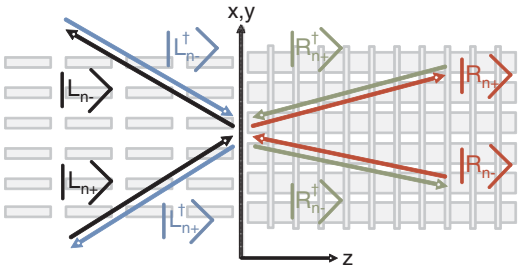

FIG. 1. (Color online) Schematic of an interface between two periodic media. The Bloch vector components tangential to the interface that are preserved are $(k_x,k_y)^T$ and $(-k_x,-k_y)^T$ for the adjoint (†) fields, respectively.

Due to the orientation of the interface as depicted in Fig. 1, we choose the transverse Bloch vector components $\mathbf{k}_\parallel = (k_x,k_y)^T$ to be equally real to maintain the fields finite at infinity. Hence the longitudinal Bloch vector component $k_{n,z} = k_{n,z}(k_x,k_y,\omega)$ will be complex in general and follows from the dispersion relation in the respective medium, which has to be solved numerically.[25] The subscript n denotes the discrete mode index; just emphasizing that there is generally an infinite set of Bloch modes applying to a particular set of fixed parameters, say, (k_x,k_y,ω). Now, by formally introducing Dirac's notation, any Bloch mode can be characterized by its eigenvalue $k_{n,z}$ and by the lattice periodic ket vector

$$|B_n\rangle(x,y,z) \equiv (E_{n,x},E_{n,y},H_{n,x},H_{n,y})^T. \tag{1}$$

Then, the complete spatial evolution of the nth mode is given by $|B_n\rangle \exp[i(\mathbf{k}_\parallel \mathbf{r}_\parallel + k_{n,z}z)]$.

Now, let us concentrate on the particular scenario shown in Fig. 1. On either side of the interface (we discuss medium $\mathcal{L}$ in the following) Fig. 1 shows four discrete sets of modes. Two of them, i.e., $|L_{n+}\rangle$ and $|L_{n-}\rangle$, are solutions to the same set of parameters, say, $(\mathbf{k}_\parallel,\omega)$. Furthermore, $|L_{n+}\rangle$ represents the modes with an energy flow in positive z direction [in absorbing materials they fulfill $\Im(k_{n,z}) > 0$] and $|L_{n-}\rangle$ are those with an energy flow in negative z direction [$\Im(k_{n,z}) < 0$]. On the other hand, $|L^\dagger_{n+}\rangle$ and $|L^\dagger_{n-}\rangle$ are the so-called adjoint fields,[37] which are solutions for the reversed tangential wave-vector component, say, $(-\mathbf{k}_\parallel,\omega)$. In contrast to the previous case, $|L^\dagger_{n+}\rangle$ represents the modes with an energy flow in negative z direction [$\Im(k_{n,z}) < 0$] and $|L^\dagger_{n-}\rangle$ are those with an energy flow in positive z direction [$\Im(k_{n,z}) > 0$].

B. Orthogonality relations

In the following, we will briefly specify the orthogonality relations between the modes as introduced above, where a detailed derivation is provided in Appendix. Here, we only give a concise summary for convenience.

According to Ref. 29, one can define a generalized inner product

$$\langle B^\dagger_n|B_m\rangle = \int\!\!\int_{\text{crosssection}} (\mathbf{E}_m \times \mathbf{H}^\dagger_n - \mathbf{E}^\dagger_n \times \mathbf{H}_m)\mathbf{e}_z dx dy \tag{2}$$

between Bloch modes of opposite transverse Bloch vector components $\mathbf{k}_\parallel$. The vector $\mathbf{e}_z$ denotes the Cartesian unit vector in z direction and the integration is performed over the cross section of one unit cell. The integrand depends solely on the tangential electromagnetic field components. As shown in Appendix, the Lorentz reciprocity theorem[38] yields the following orthogonality relations between the Bloch modes of medium $\mathcal{L}$, i.e.,

$$\langle L^\dagger_{m+}|L_{n+}\rangle = L^+_m \delta_{mn}, \tag{3}$$

$$\langle L^\dagger_{m-}|L_{n-}\rangle = -L^-_m \delta_{mn}, \tag{4}$$

$$\langle L^\dagger_{m+}|L_{n-}\rangle = 0, \tag{5}$$

$$\langle L^\dagger_{m-}|L_{n+}\rangle = 0, \tag{6}$$

where δ_{mn} denotes the Kronecker symbol, $L^\pm_m$ are normalization constants, and the minus sign in Eq. (4) is just chosen for convenience. Similar results are valid for the modes of medium $\mathcal{R}$ using different normalization constants $R^\pm_m$ in general. It has to be mentioned that the normalization constants $L^\pm_m$ as well as $R^\pm_m$ will depend on the z coordinate in general, however, this property is not relevant in the following discussion since all considerations are performed with respect to a fixed reference plane, namely the interface. Anyway, having the orthogonality relations at hand we can easily solve for the reflection and transmission coefficients at the interface between media $\mathcal{L}$ and $\mathcal{R}$.

C. Boundary value problem

Without loss of generality we assume from now on that the incident light is impinging from the left onto the interface and can be represented by a superposition of modes $|L_{n+}\rangle$. Consequently, both reflected ($|L_{n-}\rangle$) and transmitted modes ($|R_{n+}\rangle$) will be excited. According to that, the continuity of the tangential electromagnetic field components implies that

$$\sum_n i_n|L_{n+}\rangle + \sum_n r_n|L_{n-}\rangle = \sum_n t_n|R_{n+}\rangle, \tag{7}$$

with r_n and t_n being the reflection and transmission coefficients, respectively, and i_n describes the modal decomposition of the particular impinging field. The rigorous solutions for r_n and t_n can be derived by projecting Eq. (7) on $\langle R^\dagger_{k-}|$ and $\langle L^\dagger_{k+}|$ and by exploiting the orthogonality relations (3)–(6). In matrix notation, this reads as

$$\mathbf{r} = -\hat{\mathbf{a}}^{-1}\hat{\mathbf{c}}\mathbf{i}, \tag{8}$$

$$\mathbf{t} = \hat{\mathbf{d}}^{-1}\hat{\mathbf{f}}\mathbf{i}, \tag{9}$$

where the matrix elements are given by

$$a_{kn} = \langle R^\dagger_{k-}|L_{n-}\rangle, \tag{10}$$

$$c_{kn} = \langle R^\dagger_{k-}|L_{n+}\rangle, \tag{11}$$

$$d_{kn} = \langle L^\dagger_{k+}|R_{n+}\rangle, \tag{12}$$

$$f_{kn} = \langle L^\dagger_{k+}|L_{n+}\rangle = L^+_k \delta_{kn}. \tag{13}$$

To sum up, knowing the Bloch modes of both media $\mathcal{L}$ and $\mathcal{R}$, one can construct the matrices $\hat{\mathbf{a}}$, $\hat{\mathbf{c}}$, $\hat{\mathbf{d}}$, and $\hat{\mathbf{f}}$ according to Eqs. (10)–(13) and apply them to rigorously solve for the reflection and transmission coefficients of all Bloch modes excited at the interface. For the sake of completeness, we specify that the elements of the coefficient vector $\mathbf{i}$ are

calculated by projecting any incident field distribution, say $|B\rangle$, onto the modes $|L_{n+}\rangle$ which yields $i_n = \langle L_{n+}^{\dagger}|B\rangle / L_n^{+}$.

D. Fundamental mode approximation

For scenarios where the eigenmodes of both media $\mathcal{L}$ and $\mathcal{R}$ are largely matching each other, the matrices $\hat{\mathbf{a}}$, $\hat{\mathbf{c}}$, and $\hat{\mathbf{d}}$ are expected to become sparse. Hence approximate solutions can be found by contracting the description to small submatrices, which only take into account the necessary information around the matrices' diagonals. This approach resembles that used for dielectric periodic media as, e.g., photonic crystals.[31] In doing so, the size of the submatrices determines the accuracy of the approximation. However, we will restrict our following considerations to the important case where only the fundamental mode $|L_{0+}\rangle$ is impinging on the interface, i.e., $i_0 = 1, i_{n\geqslant 1} = 0$. Applying the crudest approximation, i.e., neglecting all off-diagonal elements of the matrices defined by Eqs. (10)–(13), we end up with

$$r_0 = -\frac{\langle R_{0-}^{\dagger}|L_{0+}\rangle}{\langle R_{0-}^{\dagger}|L_{0-}\rangle}, \tag{14}$$

$$t_0 = \frac{\langle L_{0+}^{\dagger}|L_{0+}\rangle}{\langle L_{0+}^{\dagger}|R_{0+}\rangle}, \tag{15}$$

for the reflection and transmission coefficients into the fundamental modes.[39] As part of this assumption, the resulting reflection and transmission coefficients $r_{n\geqslant 1}$ and $t_{n\geqslant 1}$ in all higher modes are zero. Assuming this approximation to be accurate, we then exactly mimic the situation of coupling light at the interface between two genuine homogeneous materials, i.e., coupling is exclusively determined by the fundamental eigenmodes only. Due to this fact, this approximation is called the fundamental mode approximation in the following.

III. INTERFACE BETWEEN A HOMOGENEOUS DIELECTRIC AND A METAMATERIAL: THE BLOCH IMPEDANCE

A. The bloch impedance.

After considering the general scenario of coupling between two periodically modulated media, we now proceed with the fairly special case of coupling between a homogeneous material and a periodic one. This case is of particular relevance, since it covers most practical scenarios such as MM slabs. Even more relevant, this scenario is of utmost importance since the validity of the FMA constitutes an important prerequisite for homogenization as it was discussed in Sec. I.

To continue with the specification of the relevant quantities, the eigenmodes of medium $\mathcal{L}$ become just plane waves $|P_n\rangle$. To keep the description as simple as possible, but without loss of generality, we will restrict ourselves to y-polarized incident plane waves impinging from air in the x-z plane and having a transverse wave vector $\mathbf{k}_{\parallel} = (k_x, 0)^T$. Thus

$$|P_{n+}\rangle = |P_{n-}^{\dagger}\rangle = \left(0, E_n^{\mathrm{P}}, H_n^{\mathrm{P}}, 0\right)^T, \tag{16}$$

$$|P_{n-}\rangle = |P_{n+}^{\dagger}\rangle = \left(0, E_n^{\mathrm{P}}, -H_n^{\mathrm{P}}, 0\right)^T, \tag{17}$$

with $H_n^{\mathrm{P}} = E_n^{\mathrm{P}} / Z_{\mathrm{P},n}$ and

$$Z_{\mathrm{P},n} = \frac{\sqrt{\mu_0/\epsilon_0}}{\cos\alpha + \frac{\lambda}{\Lambda_x} n} \tag{18}$$

being the transversal impedance of plane-wave mode n. Λ_x denotes the period in x direction and α is the angle of incidence.

Furthermore, assuming that the MM is mirror-symmetric with respect to both x and y direction and that it is terminated such that the unit cell is mirror symmetric with respect to z direction, similar relations[41] hold for the eigenmodes of medium $\mathcal{R}$, i.e.,

$$|R_{n+}\rangle = |R_{n-}^{\dagger}\rangle = \left(E_{n,x}^{\mathrm{B}}, E_{n,y}^{\mathrm{B}}, H_{n,x}^{\mathrm{B}}, H_{n,y}^{\mathrm{B}}\right)^T, \tag{19}$$

$$|R_{n-}\rangle = |R_{n+}^{\dagger}\rangle = \left(E_{n,x}^{\mathrm{B}}, E_{n,y}^{\mathrm{B}}, -H_{n,x}^{\mathrm{B}}, -H_{n,y}^{\mathrm{B}}\right)^T. \tag{20}$$

Now, we plug Eqs. (16)–(20) with $n = 0$ into Eq. (14), which determines r_0 in the fundamental mode approximation. In the following, we will omit the subscript "$n = 0$" from all field components, i.e., $E_0^{\mathrm{P}} \to E^{\mathrm{P}}$ and $E_{0,x}^{\mathrm{B}} \to E_x^{\mathrm{B}}$ and $Z_{\mathrm{P},0} \to Z_{\mathrm{P}}$, keeping in mind that we map everything to the forward propagating fundamental modes of both media $|P_{0+}\rangle$ and $|R_{0+}\rangle$, respectively. Now, explicitly evaluating the numerator of r_0 according to Eq. (14) we get without any further approximation ($\|\cdots\| = C^{-1}\int\int dxdy$ denotes the cross section average with C being the cross section area):

$$\begin{aligned}
\langle R_{0-}^{\dagger}|L_{0+}\rangle &= \iint dxdy \left[\mathbf{E}^{\mathrm{P}} \times \mathbf{H}^{\mathrm{B}} - \mathbf{E}^{\mathrm{B}} \times \mathbf{H}^{\mathrm{P}}\right]_z \\
&= \iint dxdy \left[E_y^{\mathrm{B}} H^{\mathrm{P}} - E^{\mathrm{P}} H_x^{\mathrm{B}}\right] \\
&= C\left(H^{\mathrm{P}} \left\| E_y^{\mathrm{B}} \right\| - E^{\mathrm{P}} \left\| H_x^{\mathrm{B}} \right\|\right) \\
&\equiv C\left(Z_{\mathrm{P}}^{-1} - Z_{\mathrm{B}}^{-1}\right) E^{\mathrm{P}} \left\| E_y^{\mathrm{B}} \right\|,
\end{aligned}$$

where we have introduced the tangential Bloch impedance of the MM

$$Z_{\mathrm{B}} = \frac{\left\| E_y^{\mathrm{B}} \right\|}{\left\| H_x^{\mathrm{B}} \right\|} \tag{21}$$

as the ratio between the averaged tangential electric and magnetic field components. Applying the analog procedure also to the denominator of Eq. (14), we get

$$\langle R_{0-}^{\dagger}|L_{0-}\rangle = -C\left(Z_{\mathrm{P}}^{-1} + Z_{\mathrm{B}}^{-1}\right) E^{\mathrm{P}} \left\| E_y^{\mathrm{B}} \right\|.$$

A very similar analysis can be also performed for the transmission coefficient t_0, but a detailed derivation will be omitted here. We find the final expressions for the reflection and transmission coefficients to be

$$r_0 = \frac{Z_{\mathrm{B}} - Z_{\mathrm{P}}}{Z_{\mathrm{B}} + Z_{\mathrm{P}}}, \tag{22}$$

$$t_0 = \frac{2Z_{\mathrm{B}}}{(Z_{\mathrm{B}} + Z_{\mathrm{P}})} \frac{E^{\mathrm{P}}}{\left\| E_y^{\mathrm{B}} \right\|}. \tag{23}$$

Most strikingly, Eqs. (22) and (23) are formally identical to the reflection/transmission coefficients at an interface between two genuine homogeneous media[42] provided that one uses the Bloch impedance as defined above to characterize the periodic medium $\mathcal{R}$.

Let us briefly organize our thoughts. It turns out that the calculation of the FMs transmission and reflection coefficients

t_0 and r_0 according to Eqs. (22) and (23) is fully equivalent to the usage of Eqs. (14) and (15) that is nothing else than the FMA in the context of a Bloch mode description. It has to be mentioned that the presented coincidence between these two descriptions is not self-evident.[43] On the one hand, it is methodologically interesting, as we believe, since it brings together two different perspectives to look at metamaterials: a periodic medium perspective (generally dealing with multiple Bloch modes) and a homogeneous medium perspective (dealing with effective wave parameters as the propagation constant and the impedance). On the other hand, and this is even more important, it may serve as a benchmark to evaluate the conditions that are prerequisite for homogenization. In other words, the validity of the FMA in comparison with the rigorous solution according to Eqs. (8) and (9) can be used to either justify or reject the assignment of effective wave parameters and, in particular, an impedance. This problem is the subject of the following paragraph and it will be dealt with by means of a specific example.

Finally, a subtle fact has to be discussed. In the current discussion, we have assumed the referential medium $\mathcal{L}$ to be a homogenous isotropic dielectric. Without having examined it in more detail, the coincidence between Eqs. (14) and (15) and Eqs. (22) and (23) (and hence the usage of the Bloch impedance) is specific to this situation. It will be repealed as soon as the referential medium becomes another periodic medium. Nevertheless, Eqs. (14) and (15) [but not Eqs. (22) and (23)] may be applicable as well, which simply expresses these equations to be the more general ones detached from the question of the participating media.

B. Swiss cross metamaterial

In the following, we will substantiate the above findings along a particular example in analyzing a Swiss cross (SC) MM[44,45] as representative for the important class of stacked MMs in detail. In particular, we will provide a fundamental guideline how to meet the FMA (being a prerequisite for homogenization) while simultaneously maintaining the dispersive features of interest. To this end, we will consider the interface between air and a SC MM in a frequency domain where the longitudinal wave vector is negative (left-handed behavior). The structure layout is depicted in Fig. 2. All geometrical parameters are given in the caption. The functional element of the SC consists of a nanostructured Au-MgO-Au stack, which is completely embedded in a host material to separate the distinct SC unit cells. The structure is periodic in all spatial dimensions and the period in z direction Λ_z will be subject to variation. It will be chosen sufficiently large such that pronounced nearest-neighbor interactions, often at the origin of fascinating effects,[46,47] are suppressed. Variation of Λ_z only changes the thickness of the host material layer. The thickness of the Au-MgO-Au stack is fixed. Hence the filling fraction of the SC element with respect to the z direction can be controlled. In the following, we assume the SC to be terminated symmetrically right in the middle of the host material layer.

Before going into the detailed analysis of the coupling problem, we first examine the dispersion relation of the fundamental mode of the SC structure. Figures 2(b) and 2(c) show the real and imaginary part of $k_z(\omega)$ for propagation

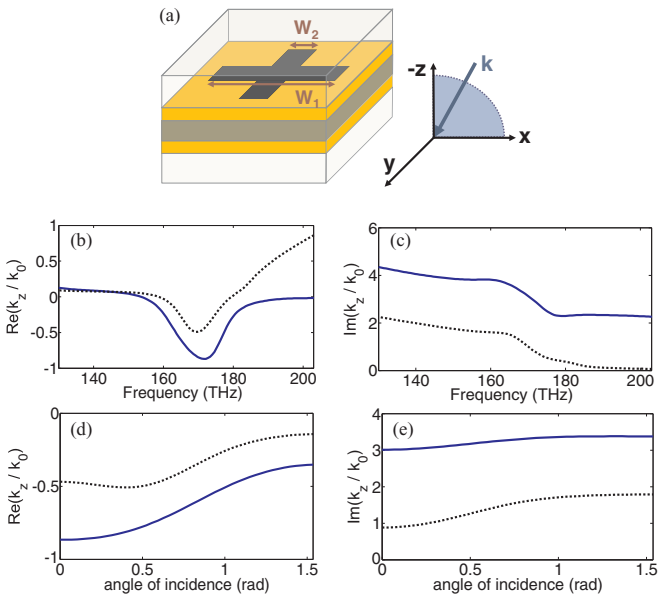

FIG. 2. (Color online) (a): Schematic of the basic setup. The incident field is polarized in y direction whereas its wave vector lies in the x-z plane such that $\mathbf{k} = (k_x,0,k_z)^T$ in general. The Swiss cross structure consists of a MgO layer ($n = 1.73$, thickness is 54 nm) sandwiched between two layers of gold (thickness is 44 nm, permittivity according to Ref. 40). The remaining parameters are $W_1 = 310$ nm, $W_2 = 90$ nm, and the lateral period is 600×600 nm^2. The entire nanostructure is embedded in a host material with refractive index of $n = 1.4$. The period in z direction will be subject to variation. (b) and (c) Dispersion relation $k_z(\omega)$ of the fundamental Bloch mode with $\mathbf{k}_\parallel = (0,0)^T$ propagating in positive z direction. (d) and (e) Dispersion relation $k_z(k_x)$ of the fundamental mode for a fixed frequency of 170 THz. The blue solid and black dotted curves correspond to a period in z direction of $\Lambda_z = 230$ and 600 nm, respectively.

along z, i.e., $\mathbf{k}_\parallel = 0$. The period Λ_z will be either 230 (blue solid lines) or 600 nm (black dotted lines), corresponding to a high- or low-filling fraction in the following discussion. Any period in-between could have been equally chosen. The corresponding dispersion relations continuously settle in-between the two representatively chosen periods. In both cases, there is a narrow frequency region (around the resonance position of 170 THz) where the real part of the propagation constant k_z becomes negative. As expected, the resonance is less pronounced for $\Lambda_z = 600$ nm, but also the attenuation [$\propto \Im(k_z)$] is decreased. For the sake of completeness, Figs. 2(d) and 2(e) also provide the angular dispersion for a fixed frequency of 170 THz. The maximum angle of $\alpha = \pi/2$ corresponds to grazing incidence of the illuminating plane wave and hence this value corresponds to $k_x = 3.56\ \mu\text{m}^{-1}$ for the transversal Bloch vector component. Obviously, $\Re(k_z)$ remains negative throughout the whole angular range.

Now, we proceed with the coupling problem, where Fig. 3 provides the necessary information. First, we concentrate on r_0 and t_0. The blue circles (black squares) show $|r_0|$ and $|t_0|$ according to Eqs. (22) and (23) for periods Λ_z equal to 230 nm (600 nm). Moreover, Figs. 3(a), 3(b), 3(e), and 3(f) also display results of rigorous calculations for r_0 and t_0.

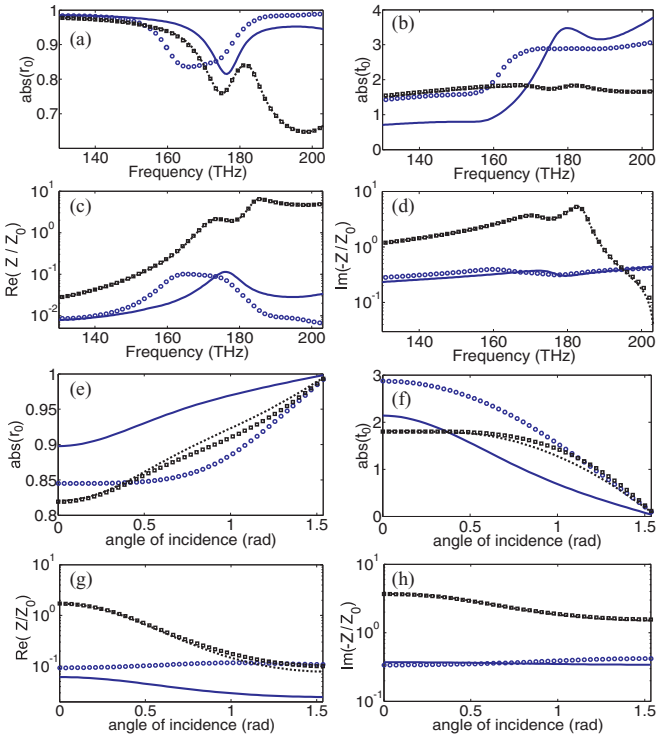

FIG. 3. (Color online) Modulus of the reflection (a) and transmission coefficient (b) in the fundamental modes $|L_{0-}\rangle$ and $|R_{0+}\rangle$ and real (c) and imaginary part (d) of the tangential Bloch impedance associated with $|R_{0+}\rangle$ for normal incidence as a function of frequency. Modulus of the reflection (e) and transmission coefficient (f) in the fundamental modes $|L_{0-}\rangle$ and real (g) and imaginary part (h) of the tangential Bloch impedance associated with $|R_{0+}\rangle$ at a frequency of 170 THz as a function of the angle of incidence. The results have been obtained by using the approximate formulas Eqs. (21)–(23). The longitudinal period of the Swiss cross unit cell amounts to $\Lambda_{z,1} = 230$ nm (blue circles) and $\Lambda_{z,2} = 600$ nm (black squares). For comparison, the results of rigorous calculations are shown by blue solid ($\Lambda_{z,1}$) and black dotted lines ($\Lambda_{z,2}$).

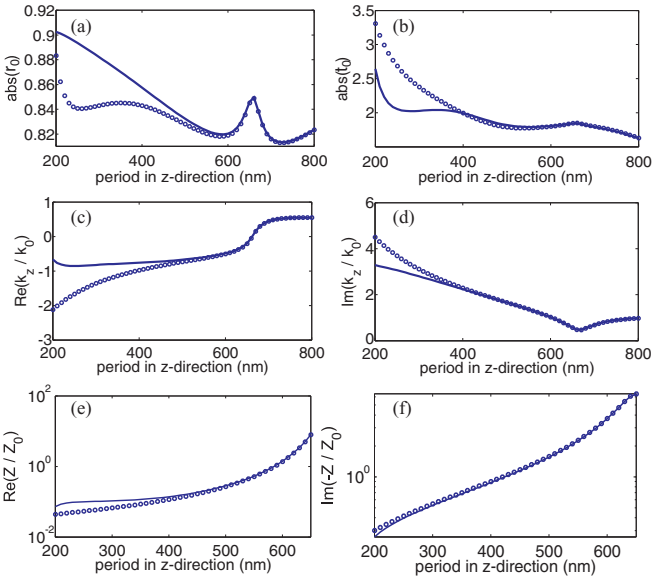

FIG. 4. (Color online) Modulus of the reflection (a) and transmission coefficient (b) in the fundamental modes $|L_{0-}\rangle$ and $|R_{0+}\rangle$, for normal incidence at 170 THz as a function of the longitudinal period. The circles represent the approximate solutions according to Eqs. (14) and (15) and the solid lines the rigorous results. (c) and (d) k_z and (e) and (f) impedance as functions of the longitudinal period. The solid lines are the propagation constants and the Bloch impedance of the fundamental Bloch mode, whereas the circles are the outcome of a parameter retrieval procedure applied to the single-layer SC structure.

For both normal and oblique incidence, the quality of the approximative solutions is clearly better for $\Lambda_z = 600$ nm.

For the sake of completeness, we also provide the normalized tangential Bloch impedances Z_B/Z_0 (with $Z_0 = \sqrt{\mu_0/\epsilon_0}$) for all considered scenarios. Here, for comparison, the impedance retrieved from reflection data $Z/Z_0 = (1 + r_0)/(1 - r_0)$ is also shown where the logarithmic scale improves the visibility. As before, it can be clearly recognized that a smaller filling fraction (longitudinal period larger than about 400 nm) leads to a reasonable agreement.

To further verify this statement, we have additionally calculated r_0 and t_0 for normal incidence at 170 THz as a function of the longitudinal period Λ_z. Figures 4(a) and 4(b) clearly evidence the suggested tendency that the accuracy of Eqs. (22) and (23) increases the smaller the filling fraction is.

The dependence of the scattering data on the longitudinal period Λ_z suggests that for small periods, higher order Bloch modes are excited. For small distances between the interface and the SC nanostructure, the optical near field becomes more complicated where also the lateral field distribution of the fundamental Bloch mode is affected.[48] Hence the mode mismatch between the exciting plane wave and the fundamental MM Bloch mode increases so that higher order modes in both media get noticeably excited. On the contrary, if the filling fraction is sufficiently small such that the interface is beyond the near-field range of the subwavelength nanostructure, the lateral field distribution of the fundamental Bloch mode converges toward a plane wave. This argument is verified by looking at the Fourier (plane wave) components of the fundamental Bloch mode for the two cases of large ($\Lambda_z = 230$ nm) and small ($\Lambda_z = 600$ nm) filling fractions, displayed in Fig. 5. It is evident that a small longitudinal period (large filling fraction) evokes a quite large mode mismatch.

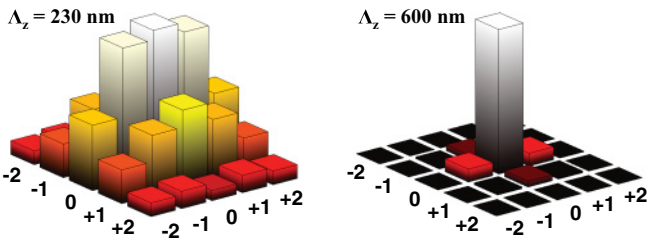

FIG. 5. (Color online) Comparison of the tangential field amplitude distribution of the fundamental Bloch mode of the SC structure in terms of its Fourier harmonics (denoted by the integer numbers). Both representations are normalized to the zeroth order Fourier harmonic. The frequency is set to 170 THz.

C. Impact on the parameter retrieval procedure

Finally, we compare the Bloch mode approach with the parameter retrieval procedure.[49] This retrieval procedure for a single layer of the current SC structure inherently leads to an effective propagation constant $k_{z,\mathrm{retr}}$ and an effective impedance Z_{retr}. Of course, the method itself does not initially require the FMA to be justified. Consequently, it appears worthwhile to investigate what the retrieved effective parameters really are. For that purpose, both retrieved parameters are compared with the propagation constant k_z and the impedance Z_{B} of the fundamental Bloch mode in Figs. 4(c)–4(f), respectively. As soon as the coupling into the MM gets dominated by the fundamental mode of each structure with an increasing period, Λ_z, $k_{z,\mathrm{retr}}$, and Z_{retr} converge towards the fundamental Bloch mode data k_z and Z_{B}, respectively.

If the FMA is not justified, the retrieved parameters $k_{z,\mathrm{retr}}$ and Z_{retr} can exhibit almost arbitrary values and cannot be linked to any modal property in general. For lossy systems, it can be easily shown that both parameters, $k_{z,\mathrm{retr}}$ and Z_{retr}, always converge with an increasing number of unit cells in propagation direction. The effective propagation constant $k_{z,\mathrm{retr}}$ converges to the propagation constant of the FM.[50] The effective impedance Z_{retr} converges to the impedance of the half space,[24] which cannot be related to a single Bloch mode. The situation gets more involved for lossless systems. Even if the propagation is dominated by the FM only, but evanescent modes still contribute to the coupling, unphysical results are expected. Consider, for example, a weakly (or non) absorbing slab of a specific nanostructure where pronounced Fabry-Perot resonances appear. For sufficiently small meta-atom size, these Fabry-Perot resonances are solely associated to the FM, whereas the artificial resonances and antiresonances observed in the effective (material) parameters[51] can be attributed to a nonvanishing contribution of higher order Bloch modes.

To sum up, provided that the filling fraction is sufficiently small, i.e., the longitudinal period Λ_z exceeds a value of about 400 nm in our current configuration, the MM can be considered entirely homogenous in the sense defined above. All properties of interest can be fully extracted from a single Bloch mode. Light evolution in the bulk MM can be derived from the Bloch mode dispersion relation, and the coupling at the interface is governed by the electric and magnetic fields of that mode there. Effective wave properties as retrieved from an inversion of the reflection and transmission coefficients entirely agree with the Bloch mode properties. However, the formalism itself can also be used to describe the coupling of light between MMs in a regime where the MMs cannot be considered homogenous. A simplification, however, can always be introduced by considering only a few Bloch modes to be involved in the process. This will be demonstrated in the following section.

IV. METAMATERIAL SLAB SURROUNDED BY A DISSIMILAR METAMATERIAL: NUMERICAL EXAMPLE

In Sec. II, the procedure to deal with the most general case of coupling between two MMs has already been outlined. Thus, in the current section we want to demonstrate the power and versatility of this approach along a genuine numerical example. For that purpose one has to remember that Eqs. (8) and (9) provide the rigorously calculated reflection and transmission coefficients in terms of the profiles of all Bloch modes supported by media $\mathcal{L}$ and $\mathcal{R}$. Again concentrating on the reflection and transmission coefficients into the fundamental modes, it is expected that these coefficients are well defined by a finite number of Bloch modes only (see discussion in Sec. II). The precise number will depend, of course, on the mode-mismatch between both media. A moderate mismatch between the modal basis of both media at the interface will result in a quite small number and vice versa.

In the following, we will probe the performance of the outlined procedure and, in particular, the applicability of the fundamental mode approximation (FMA) according to Eqs. (14) and (15). Instead of reconsidering the single interface scenario, we have now chosen a SC slab embedded in a bulk fishnet MM to perform that benchmark test. Treating this issue is the key step toward the study of an arbitrary stack consisting of different meta or natural materials. The fishnet structure is sketched in the inset of Fig. 6 and the geometrical parameters are given in the figure caption.

The SC structure is identical to that used in the previous section and the longitudinal period was set to $\Lambda_z = 230$ nm, which is likewise the thickness of the SC slab. Again, the frequency is chosen to be in the left-handed domain of the SC MM, which is operated at the resonance frequency of 170 THz. The fishnet's design is chosen such that a similar resonance occurs at the same frequency. Thus we study here the light interaction between two left-handed media.

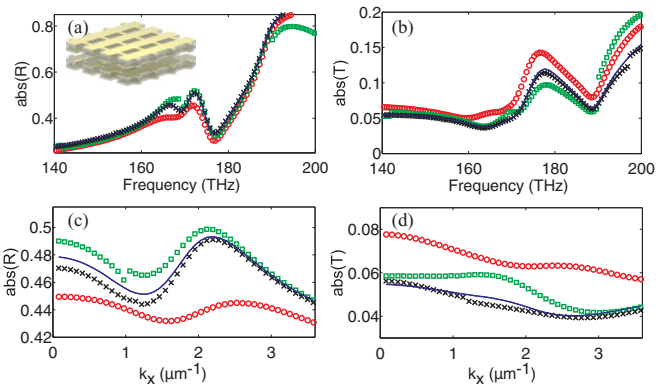

FIG. 6. (Color online) Reflection and transmission at a Swiss cross MM slab embedded between a fishnet MM. Modulus of R and T for normal incidence as a function of frequency (a) and (b) and at a frequency of 170 THz as a function of the transversal Bloch vector component k_x of the incident mode (c) and (d), respectively. The blue, solid lines are the rigorous results. The symbols represent approximate solutions taking into account a different number of modes: circles 1 (1), squares 5 (9), and crosses 15 (21). The numbers in brackets are those for oblique incidence. The fishnet's functional element consists of a Ag-MgO-Ag stack completely embedded in a host material ($n = 1.4$). The geometrical parameters are as follows: the thickness of the thick (thin) wire is 345 nm (155 nm), the permittivity of Ag is according to Ref. 52, the refractive index of MgO is 1.73, the thickness of Ag (MgO) layer is 48 nm (42 nm), the lateral period is 600×600 nm^2, and the z period $\Lambda_z = 200$ nm.

Considering the reflection and transmission properties of the SC slab, we can immediately write the overall reflection and transmission coefficients as

$$R = r_0 + \frac{t_0 t_0' r_0' \exp(2ik_z\Lambda_z)}{1 - r_0'^2 \exp(2ik_z\Lambda_z)}, \quad T = \frac{t_0 t_0' \exp(ik_z\Lambda_z)}{1 - r_0'^2 \exp(2ik_z\Lambda_z)}.$$

The primed and unprimed lower case reflection and transmission coefficients are those calculated at the single interface from the fishnet into the SC MM and vice versa. It has to be mentioned, that r_0, t_0 and r_0', t_0' represent the data of the fundamental modes only, but the number of modes used to calculate them [according to Eqs. (8)–(13)] will be subject to variations in the following discussion. On the contrary, the propagation through the thin SC slab, the height of which corresponds to a single period, is assumed to be completely governed by the fundamental mode. The results obtained will prove that this assumption is well justified. The relevant results are displayed in Fig. 6, i.e., R and T both for normal incidence as a function of the frequency [see Figs. 6(a) and 6(b)] and at a frequency of 170 THz as a function of the transverse wavevector $\mathbf{k}_\parallel = (k_x,0)^T$ [see Figs. 6(c) and 6(d)]. Comparing the FMA (red circles) with the rigorous results (blue solid lines), where all Bloch modes of both media are taken into account, it can be recognized that the FMA reproduces the main features only on qualitative grounds. Quantitatively, however, the FMA's predictions may differ by up to 25% from the rigorous results. Increasing the number of Bloch modes to built up the matrices defined by Eqs. (10)–(13), it can be observed in Fig. 6 that the results are converging across the entire spectral region. For oblique incidence the symmetry with respect to the x direction is broken resulting in a larger number of modes in both media participating in the coupling process. For that reason, an adequate convergence is only obtained with more modes than in the case of normal incidence. At first glance, the number of modes to achieve a satisfying convergence seems to be quite large. However, by using a plane-wave basis[29] rather than the Bloch mode approach, hundreds of basis states would be required to get the same accuracy.

It has to be admitted that the accuracy of the solution does not increase strictly monotonically with the number of Bloch modes taken into account. This might be attributed to the particular sorting of the Bloch modes one has chosen, because there is no *a priori* information about the importance of a particular mode with respect to coupling. In our calculations we have sorted the Bloch modes with respect to the modulus of the imaginary part of the propagation constants. Nevertheless, independent of that detail the overall convergence is always ensured.

V. CONCLUSION

In conclusion, we have provided a self-consistent and comprehensive description to analyze the reflection and transmission of light at an interface between two absorbing media composed of periodically arranged unit cells in terms of their Bloch eigenmodes. The formalism itself is rather general, but it unfolds most notably its strength when applied to MMs that may be homogenized. To this end, a homogeneous MM, as we wish to understand it here, is characterized by the property that light propagation therein and light coupling to an adjacent material is governed by the dispersion relation and the field profile of a single Bloch mode. If both conditions hold, all effective wave parameters as, e.g., the longitudinal wave vector and the impedance, can be entirely related to this Bloch mode, which is in analogy to an homogeneous optical, e.g., an anisotropic material.

It was shown that if the MM cannot be considered homogeneous multiple Bloch modes are involved in the coupling process. Then, the impedances as retrieved either from the reflection coefficient of a single interface or from the spatial field average of the fundamental Bloch mode do not coincide. A successful homogenization basically requires that the profile of the Bloch mode at the interface, and only there, has to resemble a plane wave. For deviating field distributions, higher order Bloch modes (and similarly higher order plane waves) are required to satisfy the boundary conditions at the interface.

This entails that the fundamental Bloch mode does not need to resemble a plane wave everywhere. If this would be the case, the interesting dispersive effects that make MMs so appealing could not have been witnessed. In contrast, the MM we have analyzed still possesses the dispersive effects it has been intentionally designed for, e.g., lefthandness, negative refraction, and anomalous diffraction, since close to the actual metallic nanostructure the field strongly deviates from a plane wave. Hence this concept can be applied to all stacked MMs with fixed lateral periods where the longitudinal period of the meta-atom arrangement can be made sufficiently large. Of course, this entails a trade-off between strong dispersive effects and homogenization and hence it requires a careful design in which both aspects need to be balanced. It is evident that the present formalism is not restricted to a single MM film but can be likewise applied to a sequence of different meta and natural material films.

ACKNOWLEDGMENTS

This work was partially financially supported by the Federal Ministry of Education and Research via the project Metamat and PhoNa, the Deutsche Forschungsgemeinschaft (Grant No. RO 3640/1-1), and the Thuringian State Government via the project MeMa. P. Lalanne acknowledges a Carl Zeiss Visiting Professorship. The authors acknowledge financial support from the bilateral French-German program PROCOPE under Grant Nos. 21956SD and 50076916. W. Śmigaj acknowledges a fellowship from the Triangle de la Physique.

APPENDIX: BLOCH MODE ORTHOGONALITY

In the following, we derive the orthogonality relations of Bloch modes of a periodic but absorbing medium. Therefore we start with Maxwell's equations in a medium without sources. Using a Cartesian coordinate system (x,y,z), they read as

$$\nabla \times \mathbf{E}(\mathbf{r},\omega) = i\omega\hat{\mu}(\mathbf{r},\omega)\mathbf{H}(\mathbf{r},\omega), \tag{A1}$$

$$\nabla \times \mathbf{H}(\mathbf{r},\omega) = -i\omega\hat{\epsilon}(\mathbf{r},\omega)\mathbf{E}(\mathbf{r},\omega). \tag{A2}$$

Both the permeability and permittivity tensors $\hat{\mu}(\mathbf{r})$ and $\hat{\epsilon}(\mathbf{r})$ are spatially periodic. Now, following the derivation of Ref. 29, one can show that the relation

$$\iint_{\partial V} (\mathbf{E}_2 \times \mathbf{H}_1 - \mathbf{E}_1 \times \mathbf{H}_2) \cdot d\mathbf{S} = i(\omega_1 - \omega_2) \iiint_V \left(\mathbf{E}_1^T \hat{\epsilon} \mathbf{E}_2 - \mathbf{H}_1^T \hat{\mu} \mathbf{H}_2\right) dV \qquad \text{(A3)}$$

is fulfilled for $\mathbf{E}_1$ and $\mathbf{H}_1$ ($\mathbf{E}_2$ and $\mathbf{H}_2$), representing the electric and magnetic field vectors of any monochromatic field distribution that is solution to Eqs. (A1) and (A2) at frequency ω_1 (ω_2). The only assumption one has to make for the derivation of Eq. (A3) is that the underlying materials are reciprocal, i.e., $\hat{\epsilon} = \hat{\epsilon}^T$ and $\hat{\mu} = \hat{\mu}^T$.

In what follows, Eq. (A3) is applied to the eigenmodes—the Bloch modes—of the respective medium. Using Dirac's notation, already introduced in the main body of the text [see Eq. (1)], any Bloch mode, say $|B(\omega,\mathbf{k}_\parallel)\rangle$, will depend on the chosen frequency ω and the chosen transversal (in x and y direction) Bloch vector component $\mathbf{k}_\parallel$ in a parametric manner. Similarly, the longitudinal component of the Bloch vector $k_{n,z}$ is also assumed to be a continuous function of $(\omega,\mathbf{k}_\parallel)$. It's nothing else than the dispersion relation of the periodic medium. Moreover, $(\omega,\mathbf{k}_\parallel)$ are real quantities whereas $k_{n,z}$ is complex in general.

Now, we are looking for the modes associated with a specific set of parameters $(\omega,\mathbf{k}_\parallel)$. There is a countable (mode index n) but infinite number of solutions. Moreover, one has to distinguish between forward $|B_{n+}\rangle$ and backward $|B_{n-}\rangle$ propagating modes with respect to z direction with associated Bloch vectors according to $\mathbf{k}_{n+} = (\mathbf{k}_\parallel, k_{n+,z})$ and $\mathbf{k}_{n-} = (\mathbf{k}_\parallel, k_{n-,z})$, respectively. Having this set of modes at hand, we now assume to have a second set of solutions related to the parameters $(\omega, -\mathbf{k}_\parallel)$. We will call them the adjoint modes. Of course, these solutions can be similarly divided into forward $|B^\dagger_{n-}\rangle$ and backward $|B^\dagger_{n+}\rangle$ propagating modes having Bloch vectors $\mathbf{k}^\dagger_{n-} = (-\mathbf{k}_\parallel, -k_{n-,z})$ and $\mathbf{k}^\dagger_{n+} = (-\mathbf{k}_\parallel, -k_{n+,z})$, respectively. The latter property, i.e.,

$$\mathbf{k}^\dagger_{n\pm} = -\mathbf{k}_{n\pm}, \qquad \text{(A4)}$$

is a direct consequence of Bloch mode reciprocity[29] and it will be essential in the following.

Now, to proceed with the derivation of the orthogonality relations, we introduce the fields of an arbitrary Bloch mode $|B_n\rangle$ and another adjoint mode $|B^\dagger_m\rangle$ into Eq. (A3). The integration is carried out over one unit cell in x and y direction and the frequencies are specified as $\omega_1 = \omega_2 = \omega$. In z direction, the integration volume is limited by the planes z and $z + z_0$, with z_0 being any real and positive quantity. Due to the fact that the chosen modes have an opposite transversal Bloch vector component, the integration kernel of Eq. (A3) will be strictly periodic with respect to the transversal directions. Consequently, the surface integral collapses and there are only two integrals left between the planes z and $z + z_0$. Using Dirac's notation to represent the bilinear form

$$\iint_{z=z'} (\mathbf{E}_n \times \mathbf{H}^\dagger_m - \mathbf{E}^\dagger_m \times \mathbf{H}_n)_z dx dy \equiv \langle B^\dagger_m | B_n \rangle_{z'}, \qquad \text{(A5)}$$

Eq. (A3) transforms into

$$\exp\left[i(k_{n,z} + k^\dagger_{m,z})z_0\right] \langle B^\dagger_m | B_n \rangle_{z+z_0} - \langle B^\dagger_m | B_n \rangle_z = 0. \qquad \text{(A6)}$$

Thus it is immediately clear that the product $\exp\left[i(k_{n,z} + k^\dagger_{m,z})z\right] \langle B^\dagger_m | B_n \rangle_z$ does not depend on z explicitly. Furthermore, evaluating Eq. (A6) for $z_0 = \Lambda_z$ and exploiting the quasiperiodicity of the Bloch modes along the z direction, it follows that

$$\langle B^\dagger_m | B_n \rangle_z \{1 - \exp\left[i(k_{n,z} + k^\dagger_{m,z})\Lambda_z\right]\} = 0. \qquad \text{(A7)}$$

Hence if $k_{n,z} \neq -k^\dagger_{m,z}$, the bilinear form $\langle B^\dagger_m | B_n \rangle_z$ has to vanish. Only if $k_{n,z} = -k^\dagger_{m,z}$ it may be nonzero. Making use of Eq. (A4), we can immediately identify the corresponding scenarios and derive the orthogonality relations between the usual and the adjoint modes to be

$$\langle B^\dagger_{m+} | B_{n+} \rangle_z = f(z)\delta_{mn}, \qquad \text{(A8)}$$

$$\langle B^\dagger_{m-} | B_{n-} \rangle_z = -f(z)\delta_{mn}, \qquad \text{(A9)}$$

$$\langle B^\dagger_{m+} | B_{n-} \rangle_z = 0, \qquad \text{(A10)}$$

$$\langle B^\dagger_{m-} | B_{n+} \rangle_z = 0. \qquad \text{(A11)}$$

Here, δ_{mn} denotes the Kronecker symbol being uniquely zero except for $n = m$. The introduced normalization function $f(z)$ emphasizes the z dependency of the bilinear form according to Eq. (A5). It has to be mentioned that this drawback can be easily lifted just by including the respective Bloch exponentials $\exp(ik_{n,z}z)$ and $\exp(ik^\dagger_{m,z}z)$ into the definition of Eq. (A5).

*thomas.paul@uni-jena.de

†Also at: Laboratoire Photonique, Numériques et Nanosciences, Université Bordeaux 1, CNRS, Institut d'Optique, FR-33405 Talence Cedex, France.

[1] V. G. Veselago, Sov. Phys. Usp. **10**, 509 (1968).

[2] J. B. Pendry, Phys. Rev. Lett. **85**, 3966 (2000).

[3] J. B. Pendry, D. Schurig, and D. R. Smith, Science **312**, 1780 (2006).

[4] U. Leonhardt, Science **323**, 110 (2009).

[5] U. Leonhardt and T. G. Philbin, Prog. Opt. **53**, 69 (2009).

[6] M. Schmiele, C. Rockstuhl, and F. Lederer, Phys. Rev. A **79**, 053854 (2009).

[7] B. Vasić, G. Isić, R. Gajić, and K. Hingerl, Phys. Rev. B **79**, 085103 (2009).

[8] M. Schmiele, V. S. Varma, C. Rockstuhl, and F. Lederer, Phys. Rev. A **81**, 033837 (2010).

[9] C. R. Simovski, Opt. Spectrosc. **107**, 726 (2009).

[10] C. Menzel, T. Paul, C. Rockstuhl, T. Pertsch, S. Tretyakov, and F. Lederer, Phys. Rev. B **81**, 035320 (2010).

[11] V. A. Markel and J. C. Schotland, J. Opt. **12**, 015104 (2010).

[12] N. Wellander and G. Kristensson, SIAM J. Appl. Math. **64**, 170 (2003).

[13] A. Ishikawa, T. Tanaka, and S. Kawata, Phys. Rev. Lett. **95**, 237401 (2005).
[14] J. Zhou, Th. Koschny, M. Kafesaki, E. N. Economou, J. B. Pendry, and C. M. Soukoulis, Phys. Rev. Lett. **95**, 223902 (2005).
[15] X. Zhang, M. Davanço, Y. Urzhumov, G. Shvets, and S. R. Forrest, Phys. Rev. Lett. **101**, 267401 (2008).
[16] D. Seetharamdoo, R. Sauleau, K. Mahdjoubi, and A.-C. Tarot, J. Appl. Phys. **98**, 063505 (2005).
[17] T. Paul, C. Rockstuhl, C. Menzel, and F. Lederer, Phys. Rev. B **79**, 115430 (2009).
[18] The fundamental mode prevails against all other Bloch modes in terms of attenuation, polarization, and symmetry and therefore its choice depends on the particular coupling conditions.
[19] C. R. Simovski and S. A. Tretyakov, Phys. Rev. B **75**, 195111 (2007).
[20] C. R. Simovski, Metamaterials **1**, 62 (2007).
[21] K. Sakoda, *Optical Properties of Photonic Crystals* (Springer, Berlin, 2001).
[22] C. Rockstuhl, C. Menzel, T. Paul, T. Pertsch, and F. Lederer, Phys. Rev. B **78**, 155102 (2008).
[23] X. Zhang, M. Davanco, Y. Urzhumov, G. Shvets, and S. R. Forrest, Phys. Rev. Lett. **101**, 267401 (2008).
[24] J. Yang, C. Sauvan, T. Paul, C. Rockstuhl, F. Lederer, and P. Lalanne, Appl. Phys. Lett. **97**, 061102 (2010).
[25] Z.-Y. Li and K.-M. Ho, Phys. Rev. B **68**, 245117 (2003).
[26] P. Lalanne, Phys. Rev. B **58**, 9801 (1998).
[27] B. Gralak, S. Enoch, and G. Tayeb, J. Opt. Soc. Am. A **19**, 1547 (2002).
[28] T. Paul, C. Menzel, C. Rockstuhl, and F. Lederer, Adv. Mater. **22**, 2354 (2010).
[29] G. Lecamp, J. P. Hugonin, and P. Lalanne, Opt. Express **15**, 11042 (2007).
[30] W. Śmigaj, P. Lalanne, J. Yang, T. Paul, C. Rockstuhl, and F. Lederer, Appl. Phys. Lett. **98**, 111107 (2011).
[31] F. J. Lawrence, L. C. Botten, K. B. Dossou, C. M. de Sterke, and R. C. McPhedran, Phys. Rev. A **80**, 023826 (2009).
[32] R. Biswas, Z. Y. Li, and K. M. Ho, Appl. Phys. Lett. **84**, 1254 (2004).
[33] B. Momeni, A. Asghar Eftekhar, and A. Adibi, Opt. Lett. **32**, 778 (2007).
[34] B. Momeni, M. Badieirostami, and A. Adibi, J. Opt. Soc. Am. B **24**, 2957 (2007).
[35] W. Śmigaj and B. Gralak, Phys. Rev. B **77**, 235445 (2008).
[36] F. J. Lawrence, L. C. Botten, K. B. Dossou, R. C. McPhedran, and C. M. de Sterke, Phys. Rev. A **82**, 053840 (2010).
[37] P. Y. Chen, R. C. McPhedran, C. M. de Sterke, C. G. Poulton, A. A. Asatryan, L. C. Botten, and M. J. Steel, Phys. Rev. A **82**, 053825 (2010).
[38] A. W. Snyder and J. D. Love, *Optical Waveguide Theory* (Chapman and Hall, New York, 1983).
[39] Actually, neglecting all higher order BM overlaps of type $\langle R^{\dagger}_{k-}|L_{n\pm}\rangle$ and $\langle L^{\dagger}_{k+}|R_{n+}\rangle$ with $k \neq n$ is a very demanding assumption, which can be refined in order to achieve the same approximations for r_0 and t_0 as it is discussed in Ref. 30.
[40] P. B. Johnson and R. W. Christy, Phys. Rev. B **6**, 4370 (1972).
[41] P. Lalanne and J. P. Hugonin, IEEE J. Quantum Electron. **39**, 1430 (2003).
[42] The fundamental Bloch mode $|R_{0+}\rangle$ can always be normalized to fulfill $E_y^{\mathrm{B}} = 1$.
[43] Indeed, the rigorous solution (8) and (9) of the boundary-value problem according to Eq. (7) can be written in several equivalent forms, corresponding to the projection on different complete sets, e.g., $\langle R^{\dagger}_{k+}|$ and $\langle L^{\dagger}_{k-}|$ rather than $\langle R^{\dagger}_{k-}|$ and $\langle L^{\dagger}_{k+}|$, as it was done in the text. When truncated to the contribution of the FM, however, these equivalent formulas give rise to different approximate expressions for r_0 and t_0. One alternative formula for these coefficients was derived in Ref. 30. We have found that the accuracy of the FMA description is only weakly dependent on which of these approximate solutions is chosen. In that sense, the usage of the Bloch impedance according to Eqs. (22) and (23) represents only one particular choice to integrate the properties of the fundamental Bloch mode into the calculation of the reflection and transmission coefficients.
[44] C. Helgert, C. Menzel, C. Rockstuhl, E. Pshenay-Severin, E.-B. Kley, A. Chipouline, A. Tünnermann, F. Lederer, and T. Pertsch, Opt. Lett. **34**, 704 (2009).
[45] M. Kafesaki, I. Tsiapa, N. Katsarakis, Th. Koschny, C. M. Soukoulis, and E. N. Economou, Phys. Rev. B **75**, 235114 (2007).
[46] N. Liu and H. Giessen, Angew. Chemie Int. Ed. **49**, 9838 (2010).
[47] N. Liu and H. Giessen, Opt. Express **16**, 21233 (2008).
[48] M. Burresi, D. Diessel, D. van Oosten, S. Linden, M. Wegener, and L. Kuipers, Nano Lett. **10**, 2480 (2010).
[49] D. R. Smith, S. Schultz, P. Markoˇv, and C. M. Soukoulis, Phys. Rev. B **65**, 195104 (2002).
[50] C. Rockstuhl, T. Paul, F. Lederer, T. Pertsch, T. Zentgraf, T. P. Meyrath, and H. Giessen, Phys. Rev. B **77**, 035126 (2008).
[51] J. Qi, H. Kettunen, H. Wallén, and A. Sihvola, IEEE Ant. Wireless Prop. Lett. **9**, 1057 (2010).
[52] Permittivity of silver: $\epsilon_{\mathrm{Ag}} = 1 - \omega_p^2/(\omega^2 + ig\omega)$ with $\omega_p = 1.37 \times 10^{16}\ \mathrm{s}^{-1}$ and $g = 8.5 \times 10^{13}\ \mathrm{s}^{-1}$.